

## Investigation on interlaminar shear stresses in laminated composite beam under thermal and mechanical loading

Nagaraj Murugesan<sup>a</sup> and Vasudevan Rajamohan<sup>\*</sup>

*School of Mechanical and Building Sciences, VIT University, Vellore 632 014, Tamil Nadu, India*

*(Received February 17, 2014, Revised June 13, 2014, Accepted August 22, 2014)*

**Abstract.** In the present study, the combined effects of thermal and mechanical loadings on the interlaminar shear stresses of both moderately thin and thick composite laminated beams are numerically analyzed. The finite element modelling of laminated composite beams and analysis of interlaminar stresses are performed using the commercially available software package MSC NASTRAN/PATRAN. The validity of the finite element analysis (FEA) is demonstrated by comparing the experimental test results obtained due to mechanical loadings under the influence of thermal environment with those derived using the present FEA. Various parametric studies are also performed to investigate the effect of thermal loading on interlaminar stresses generated in symmetric, anti-symmetric, asymmetric, unidirectional, cross-ply, and balanced composite laminated beams of different stacking sequences with identical mechanical loadings and various boundary conditions. It is shown that the elevated thermal environment lead to higher interlaminar shear stresses varying with the stacking sequence, length to thickness ratio, ply orientations under identical mechanical loading and boundary conditions of the composite laminated beams. It is realized that the magnitude of the interlaminar stresses along  $xz$  plane is always much higher than those of along  $yz$  plane irrespective of the ply-orientation, length to thickness ratios and boundary conditions of the composite laminated beams. It is also observed that the effect of thermal environment on the interlaminar shear stresses in carbon-epoxy fiber reinforced composite laminated beams are increasing in the order of symmetric cross-ply laminate, unidirectional laminate, asymmetric cross-ply laminate and anti-symmetric laminate. The interlaminar shear stresses are higher in thinner composite laminated beams compared to that in thicker composite laminated beams under all environmental temperatures irrespective of the laminate stacking sequence, ply-orientation and boundary conditions.

**Keywords:** composite laminates; interlaminar shear stresses; orthotropic materials; thermal environment; finite element analysis

---

### 1. Introduction

Composite materials are widely used in structures wherever light weight and high strength are the primary design drivers (Tahani 2007). Orthotropic nature of the composite materials provides wide choice of design solutions. Operating environment plays a major role in the performance parameters of structures made of composite materials. The orthotropic material properties of the

---

<sup>\*</sup>Corresponding author, Professor, E-mail: [vasudevan.r@vit.ac.in](mailto:vasudevan.r@vit.ac.in)

<sup>a</sup> M.S. (By Research) Student, E-mail: [nagaraj\\_m@hotmail.com](mailto:nagaraj_m@hotmail.com)

plies and their stacking sequence yield the interlaminar stresses. Interlaminar stresses lead to defects such as delamination and reduce the load carrying capacity and life of the laminates. Hence accurate determination of the interlaminar stresses is crucial for designing composite laminates (Matsunaga 2003). Furthermore, composite materials are degraded by environmental attack such as moisture diffusion, thermal spikes, ultraviolet radiation, and thermal oxidation, etc. The temperature effect on the fiber-matrix interface is as strong as those of the fiber treatment and resin properties. The differential thermal coefficients of composite laminae lead to internal stresses in the laminates. Such internal stresses vary with temperature variation, in some cases generates matrix cracking at very low temperatures. Hence, the investigation on thermal effects on the interlaminar shear stress distribution is important in the early design of a composite structure (Matsunaga 2004).

The classical laminated plate theory, based on the Kirchhoff hypothesis, is inaccurate for multilayered composite laminates due to the negligence of the effects of transverse shear and normal strains. Interlaminar stresses in simply supported composite plates subjected to mechanical loadings were analysed by Pagano (1969) using 3D layerwise elasticity solution. It was found that conventional plate theory leads to a very poor description of laminate response at low span-to-depth ratios, but converges to the exact solution as this ratio increases. The analysis presented is also valid in the study of sandwich plates under cylindrical bending. The interlaminar stresses generated due to uniform bending were presented using a finite-difference approximation by Salamon (1978). Even though the magnitudes of the interlaminar shear and normal stresses were relatively small, they were found to rise sharply near the free edges. Kassapoglou (1990) presented the state of stress at the free edges of composite laminates under the combination of uniaxial tension or compression, moment and out-of-plane shear and evaluated all six stresses at straight free edges of composite laminates under combination of mechanical loads. Lee and Liu (1992) presented an interlaminar stress continuity theory for analyzing composite laminates under mechanical loading. It was also concluded that the aspect ratio of the element length to the composite thickness, namely element aspect ratio, was found to play a very important role in convergence. Wu and Kuo (1993) analysed thick laminated composite plates using an interlaminar stress mixed finite element method. The local high order displacement fields were applied in the local region of interest while the global high order displacement fields were applied in the remote region. Sub-laminate-layer model using Lekhnitskii's stress functions were used for analysis of composite laminates by Lee (1994). It was concluded that the intense and localized interlaminar stresses near a particular location of the free edge depend mainly on the local values of the load parameters as suggested by Saint Venant's principle and the reciprocity relations of elasticity. Hu *et al.* (1997) presented a three-dimensional finite-element model to analyse interlaminar stresses in composite laminates with a circular hole. For two layered cross-ply laminates, the estimated interlaminar stresses were very high close to the hole and became vanishingly small within a two-ply thickness of the edge. Out-of-plane shear deformation model was presented to analyse the interlaminar shear stresses in solid composite beams by Rand (1998). The solution procedure exploited the beam slenderness to construct a finite difference numerical scheme. It was shown that the warping is a function of the loading mode. Rolfes and Rohwer (2000) presented integrated thermal and mechanical analysis of composite plates and shells. It was shown that the thermal lamination theories, assuming a linear or quadratic temperature distribution across the thickness, were well suited to capture the 3D temperature field for laminates where the direction of thermal anisotropy changes drastically from layer to layer. An iterative method was presented by Cho and Kim (2000) to analyze free edge interlaminar stresses of composite laminates subjected to

extension, bending, twisting and residual thermal loads. The interlaminar stresses near free edges in composite laminates have been analyzed by the extended Kantorovich method. Becker *et al.* (2001) analysed the localized occurrence of interlaminar stresses along the free edges of composite laminates. It was shown that the criticality of free-corner effect with regard to delamination depends on the laminate layup and the single-ply material characteristics. Displacements and interlaminar stresses of. It was shown that the transverse normal deformation effect is not negligible in the situatiolaminated composite beams subjected to a transverse loading according to global higher order deformation theories were presented by Matsunaga (2002). It was concluded that the effect of the continuity conditions of displacement components at the interface between the layers is very important to predict the true mechanical characteristics of laminates with a large number of layers. Interlaminar stresses in laminated composite arches subjected to thermal and mechanical loading were presented using global higher-order plate theory by Matsunaga (2003). The displacement distributions and transverse shear and normal stresses of simply supported multilayered composite circular arches were predicted. Finite element based zig-zag plate theories were developed by Cho and Oh (2003, 2004) and Oh and Cho (2004) to predict the mechanical, thermal, and electric behaviours fully coupledns that electric and thermal loads are applied. Simple and exact series solutions for flexure of orthotropic rectangular plates were presented by Bhaskar and Kaushik (2004) with a combination of clamped and simply supported edges. Based on superposition of double sine series solutions, arbitrarily loaded cross-ply plates with combinations of simply-supported and clamped edges were analyzed. Matsunaga (2004) compared between 2-D single-layer and 3-D layerwise theories for computing interlaminar stresses of laminated composite and sandwich plates subjected to thermal loadings. Effects of the difference of displacement continuity conditions between the three dimensional layerwise theory and the global higher order theory in multilayered composite and sandwich plates subjected to thermal loadings were investigated. Tong *et al.* (2004) presented three-dimensional finite element interlaminar stress solutions of composite laminates with resin layers under uniform axial strain. The effects of free-edge on interlaminar stresses in cross-ply and angle-ply laminates were analyzed. Murthy *et al.* (2005) derived a refined 2-node, 4 DOF/node beam element based on higher order shear deformation theory for axial-flexural-shear coupled deformation in asymmetrically stacked laminated composite beams. It was concluded that the complexity in handling the quadratic variation of the transverse displacement across the beam thickness for thick composite beams and plates is an open area of research. A finite element method for a quasi-three-dimensional problem was presented by Wu and Yan (2005) to analyse interlaminar stress distributions of composite laminates. The likely interfaces of delamination in composite laminates of different ply orientations were predicted. Kress *et al.* (2005) presented a new model to investigate the interlaminar normal stress distribution in moderately thick and singly curved laminates. This model requires in-plane strain information which could also map the kinematical effects caused by the curved laminate shape. Tahani (2007) developed a new layer wise laminated beam theory to overcome the shortcomings of plate and shell theories to evaluate the interlaminar stresses developed in laminated structures. It was concluded that the approach adopted in derivation of the equations of motion in the new beam theory is direct and straight forward similar to the theories used in developing laminated plate and shell theories. Higher order shear deformation theory was used in the thermal buckling analysis of cross-ply laminated composite beams by Aydogdu (2007). A family of sinus finite elements with a three-nodded mechanical beam finite element without considering the shear correction factors was developed by Vidal and Polit (2008) to identify the transverse shear stress of rectangular laminated beams. Furthermore mechanical tests for thin and

thick beams were presented. Interlaminar shear stresses in thick composite and sandwich composite plates were presented using Higher-order layerwise laminate theory by Plagianakos and Saravanos (2009). A semi-analytical solution using Ritz method was further implemented to yield the structural response of thick composite and sandwich composite plates. A refined sine-based finite element with transverse normal deformation for the analysis of laminated beams under thermo mechanical loads was presented by Vidal and Polit (2009). This study showed the necessity of taking into account the transverse normal effect which cannot be neglected, in particular for coupled thermomechanical problems. A generalized three-dimensional global–local theory was proposed for thick as well as thin imperfect laminated composite and sandwich plates subjected to thermo-mechanical loads by Shariyat (2010). It was concluded that the generalized three-dimensional global–local theory is capable of investigating the wrinkling phenomenon in the face sheets of the sandwich plates. Gayen and Roy (2013) presented an analytical method to determine the interlaminar stress distributions in multilayered symmetric and anti-symmetric circular tapered laminated composite beams under hygro and thermal loadings. It was concluded that the axial in-plane stresses vary with change in moisture concentration, temperature, fiber orientation of the plies in addition to the mismatch of coefficients of axial thermal and moisture expansions in each ply of the laminate. Even though numerous research works have been focused on interlaminar shear stress distribution on composite structures, the effect of thermal environment on the variation of interlaminar stresses on composite beams are yet to be explored in detail.

In this study the combined effect of thermal loading and mechanical loadings on the interlaminar shear stresses of both moderately thick and thin composite laminated beams are numerically analyzed. The finite element modelling of laminated composite beams and analysis of interlaminar stresses are performed using the commercially available software package MSC NASTRAN/PATRAN. The validity of the finite element analysis is demonstrated by comparing the results in terms of interlaminar shear stresses obtained from experimental test due to mechanical loadings under the influence of thermal environment by three point bending method. Various parametric studies are also performed to investigate the effect of thermal loading on interlaminar stresses generated in symmetric, anti-symmetric, asymmetric, unidirectional, cross-ply and balanced composite laminated beams of different stacking sequences with identical mechanical loadings and various boundary conditions.

## 2. Numerical modelling and analysis

A laminated composite beam of length  $L$ , width  $B$  and the thickness  $H$  is considered for the numerical analysis of interlaminar stress distribution under the combination of mechanical and thermal loadings. The width and thickness of the beam are considered to be significantly small compared to length of the beam. The beam consists of  $N$  number of layers with various ply orientation. The slippage between the adjacent laminae is assumed to be negligible by considering the perfect bonding between the laminae which leads to the continuous displacement and traction at each interface. Furthermore, each lamina is considered to be elastic, homogeneous and orthotropic.

The laminated composite beams of different staking sequences are modelled using the commercially available FEA software package MSC NASTRAN/PATRAN. The beam is discretized using a standard four noded QUAD4 element and each node consists of five degrees of freedom including three translational displacement along  $x$ ,  $y$ , and  $z$  axes and two rotational

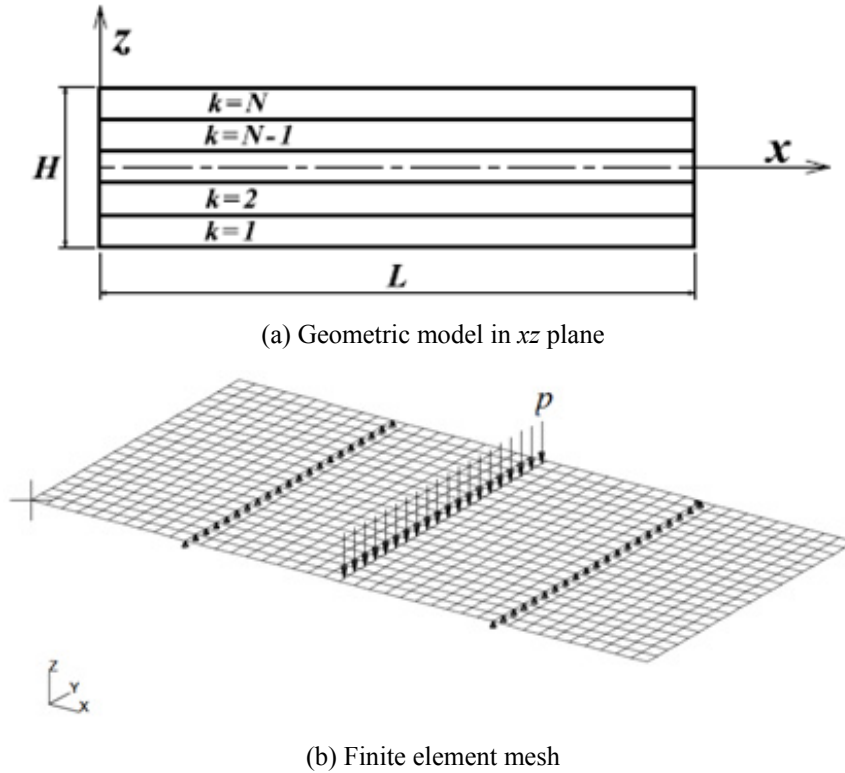


Fig. 1 Representation of a composite laminated beam

degrees of freedom with respect to  $x$  and  $y$  axes, respectively. A brief description of the procedure followed in FEA is as follows:

The geometry of the composite laminated beam of length ' $L$ ' and width ' $B$ ' in  $xy$  plane is first modeled in MSC PATRAN and discretized using 4 noded QUAD4 shell elements. The layer material properties are provided as input in the material properties option available in the software. Then the laminate modeler available in the software is used to model the composite laminate taking into account the number of layers, material properties of each layer, each layer thickness, orientation of each layer and their layup sequence of the particular configuration of composite laminated beam. The composite laminate model so developed is applied to the QUAD4 shell elements of the beam. Various boundary conditions are applied. Further, thermal load (elevated temperature) is applied simultaneously to the shell elements in addition to the mechanical loadings. The preprocessed model so developed is solved (processed) using static analysis tool available in MSC NASTRAN.

In the post processing, the stresses at all the nodes of the mid plane as well as all the layer interfaces are extracted and their maximum values are presented as normalized values.

### 3. Experimental investigation

Laboratory experiments were performed on prototype composite specimens to investigate the

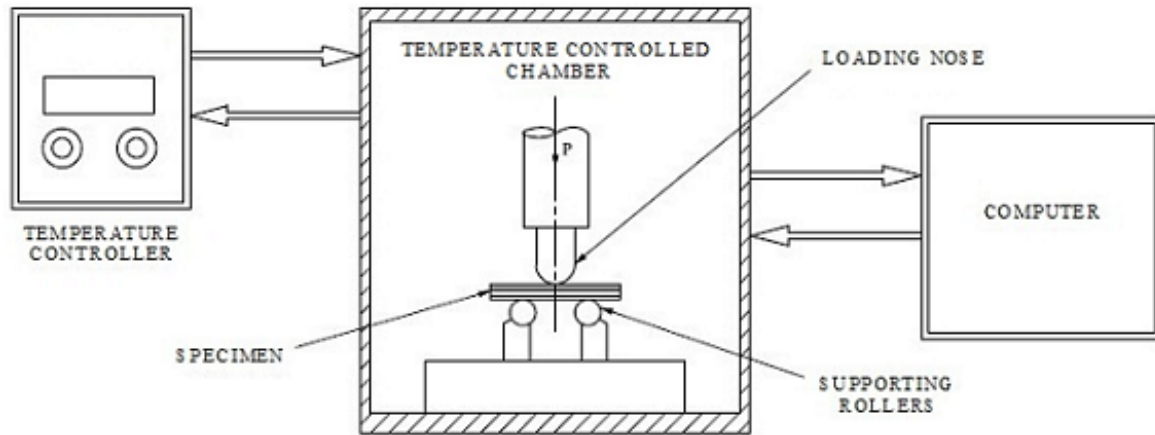


Fig. 2 Block diagram of experimental setup

effect of thermal and mechanical loadings on distribution of interlaminar shear stress. Two symmetric composite laminated beams with stacking sequences of  $[0/90]_{4S}$  and  $[0]_{16}$  are fabricated out of standard carbon-epoxy unidirectional prepreg tape T300/914C supplied by Hexcel<sup>®</sup>. The prepreg unidirectional tapes were cut to required size and stacked in the sequence required. The stacked layups were then vacuum bagged and cured in an autoclave at 175°C (heat-up rate between 2-5°C per minute) and 7 bar pressure for 1 hour and post cured for 4 hours at 190°C (Gatto *et al.* 2009). Then the autoclave was allowed to cool off naturally to room temperature. The composite laminates so obtained were then inspected, cleaned and used for preparing the test specimen of size 20 mm length and 10 mm width for testing of interlaminar shear stresses.

Computerized universal testing machine of 'Kalpak' make with thermal loading facility as shown in Fig. 2 was used for measuring the interlaminar shear stress of the specimen cut from the laminate fabricated. This universal testing machine is capable of real time data capture, display of data and test curves and save the test results. Three point bending fixture as shown in Fig. 2 is housed inside the thermal conditioning chamber which is integrated in this universal testing machine. The thermal environment inside the chamber can be digitally controlled.

The composite laminated beam test specimen was kept at the test temperature for 10 minutes before testing. The specimen is placed on the fixture as shown in Fig. 2, such that the axis of the specimen is perpendicular to the axis of the supporting rollers. The environment of the testing chamber was maintained at the required test temperature. Mechanical load was applied, in three-point bending, at a speed of 2mm/ minute until first significant load drop was observed on the load-deflection curve. The maximum load applied  $P_m$  was recorded and the maximum interlaminar stress (short beam strength) is calculated such that

$$\text{Interlaminar shear stress, } \sigma = 0.75P_m / BH \quad (1)$$

The specimens prepared with stacking sequences of symmetric cross-ply laminate  $[0/90]_{4S}$  and  $[0]_{16}$  were tested in 'Computerised Universal Testing Machine with thermal conditioning chamber' as explained and the results were recorded.

#### 4. Validation

The composite laminated beams with stacking sequences of symmetric cross-ply laminate  $[0/90]_{4S}$  and  $[0]_{16}$  are analyzed using the present finite element model. The geometry and the stacking sequences are modelled as per the experimental test specimen following ASTM D2344/D2344M.

The following orthotropic material properties of each layer at reference temperature of the above fabricated laminates are considered for finite element analysis

$$E_L = 130 \text{ GPa}, E_T = 9.5 \text{ GPa}, G_{LT} = 4.3 \text{ GPa}, G_{TT} = 3.308 \text{ GPa}, \quad (2)$$

$$\nu_{LT} = 0.32, \alpha_L = -0.18 \times 10^{-6}, \alpha_T = 30 \times 10^{-6}$$

where  $E$ ,  $G$ ,  $\nu$  and  $\alpha$  are elastic modulus, shear modulus, Poisson’s ratio and coefficient of thermal expansion respectively and the subscripts, ‘ $L$ ’ and ‘ $T$ ’ signify the direction parallel to the fibres and the transverse direction for orthotropic material.

A uniformly distributed load, ‘ $p$ ’ equivalent to the maximum applied load of each test case of experimental evaluation of the interlaminar shear stresses, along ‘ $y$ ’ direction at the mid span and on top surface of the laminated beam ( $z = +H/2$ ) is considered to be applied along with thermal loading of the test case.

Finite element analysis is performed using the static analysis tool available in FEA software package MSC NASTRAN/PATRAN. The maximum interlaminar shear stress,  $\sigma_{xz}^{(T)}$  under the combined thermal and mechanical loading are examined. The results are presented as normalized quantities defined such that

$$\bar{\sigma}_{xz}^{(T)} = \sigma_{xz}^{(T)} / (T_{ref} \alpha_o E_o) \quad (3)$$

where,  $T_{ref}, \alpha_o = 10^{-6}/K$  and  $E_o = 1 \text{ GPa}$  are reference room temperature, reference thermal expansion coefficient and reference elastic modulus, respectively.

The validity of the finite element analysis is demonstrated by comparing the results in terms of interlaminar shear stress along  $xz$  plane obtained from finite element analysis with those identified from experimental investigation and are presented in Tables 1 and 2 for the laminate stacking sequences of  $[0/90]_{4S}$  and  $[0]_{16}$ , respectively. Very good agreement is observed between the results evaluated using current FEA and the experimental tests.

Table 1 Comparison of the normalized maximum interlaminar shear stress  $\bar{\sigma}_{xz}^{(T)}$  evaluated from experimental test with those obtained using current FEA for the laminate stacking sequence  $[0/90]_{4S}$

Thermal loading, K	Normalized maximum interlaminar shear stress, $\bar{\sigma}_{xz}^{(T)}$		
	Experimental (a)	Present FEA (b)	Deviation, % [(a)-(b)]*100/(a)
297.1	256.31	250.48	2.32
323.0	226.19	220.95	2.36
348.0	205.17	200.43	2.37
373.0	174.48	170.58	2.28

Table 2 Comparison of the normalized maximum interlaminar shear stress  $\bar{\sigma}_{xz}^{(T)}$  evaluated from experimental test with those obtained using current FEA for the laminate stacking sequence  $[0]_{16}$

Thermal loading, K	Normalized maximum interlaminar shear stress, $\bar{\sigma}_{xz}^{(T)}$		
	Experimental (a)	Present FEA (b)	Deviation, % [(b)-(a)]*100/(b)
297.1	311.41	330.38	5.74
323.0	262.29	278.58	5.85
348.0	232.76	246.75	5.70
373.0	202.12	214.42	5.76

## 5. Results and discussions

The interlaminar shear stresses of a laminated structure are dependent on various factors including length, width and thickness of the beam, ply orientation, boundary conditions and the environmental temperature. The effect of ratio of length to thickness of the beam, environment temperature, stacking sequence and the boundary conditions on the variation of interlaminar shear stresses is investigated. The material and geometric properties considered for the simulation are identical with those used in the previous section.

Composite beams made of symmetric cross-ply laminate, asymmetric cross-ply composite laminate, anti-symmetric laminate, and unidirectional composite laminate with stacking sequences of  $[0/90]_{4S}$ ,  $[0/90]_8$ ,  $[0/(\pm 45)_7/0]$ ,  $[0]_{16}$ ,  $[45]_{16}$  and  $[90]_{16}$  respectively, are considered for the simulation. The variation of interlaminar shear stresses of the above laminated beams of various ratios of length ( $L$ ) to thickness ( $H$ ), ( $L/H$  ratio) under clamped-clamped, clamped-hinged and hinged-hinged boundary conditions, respectively with the combined effect of change in the environmental temperatures and the mechanical loading is studied. A uniformly distributed load, ' $p$ ' equal to 1000N/mm along ' $y$ ' direction at the mid span of the beam and on top surface of the laminated beam ( $z = +H/2$ ) is considered to be applied.

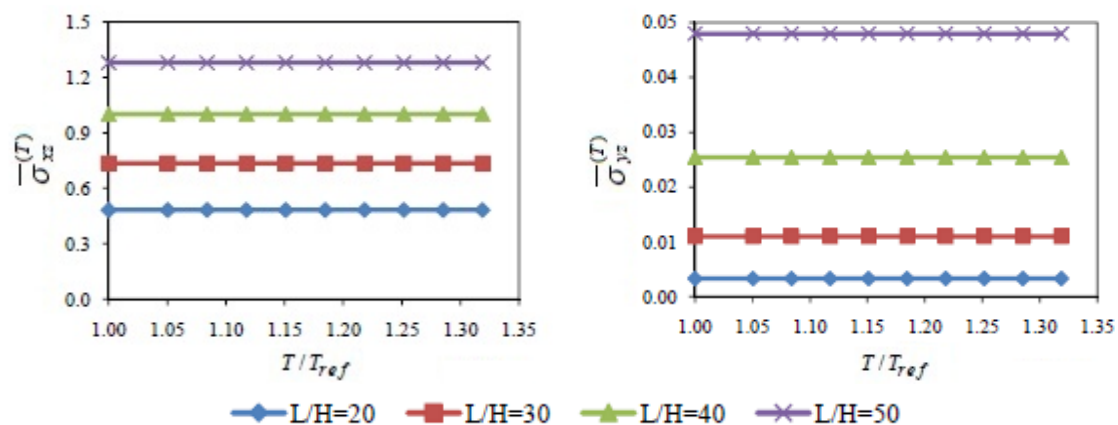


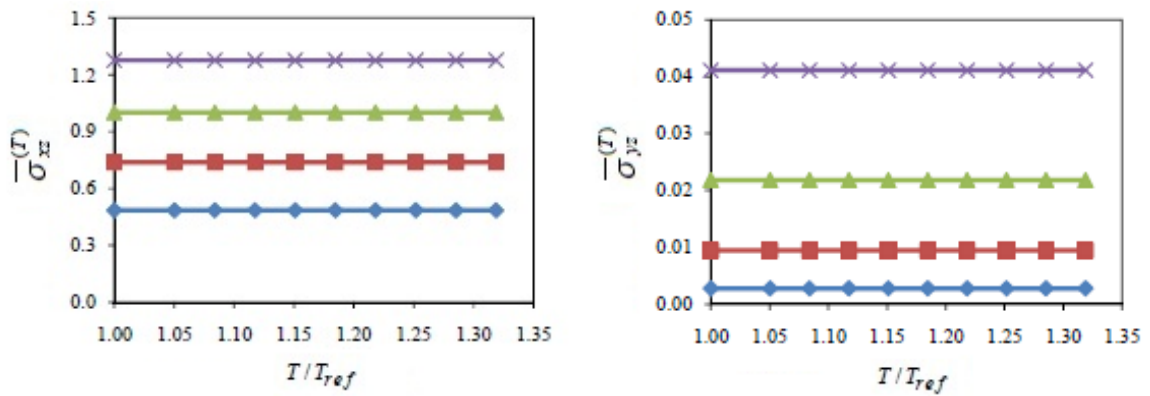
Fig. 3 Variation of normalised maximum interlaminar shear stresses (ILSS), at the interface of 4th and 5th layers of symmetric laminated composite beam with  $[0/90]_{4S}$  ply orientation along  $xz$  ( $\bar{\sigma}_{xz}^{(T)}$ ) and  $yz$  ( $\bar{\sigma}_{yz}^{(T)}$ ) planes under clamped-hinged boundary conditions

The FE analysis provides the interlaminar shear stresses and inplane shear stresses at the interfaces of all the layers of the composite laminated beam. Variation of normalised maximum interlaminar shear stresses (ILSS) along  $xz$  ( $\bar{\sigma}_{xz}^{(T)}$ ) and  $yz$  ( $\bar{\sigma}_{yz}^{(T)}$ ) planes at the interface of 4th and 5th layers of symmetric laminated composite beam with  $[0/90]_{4S}$  ply orientation under clamped-hinged boundary conditions are presented in Fig. 3. Considering the huge stress data obtained at all the nodal points along all the layer interfaces, the normalized maximum interlaminar shear and inplane shear stresses are presented in the subsequent discussions.

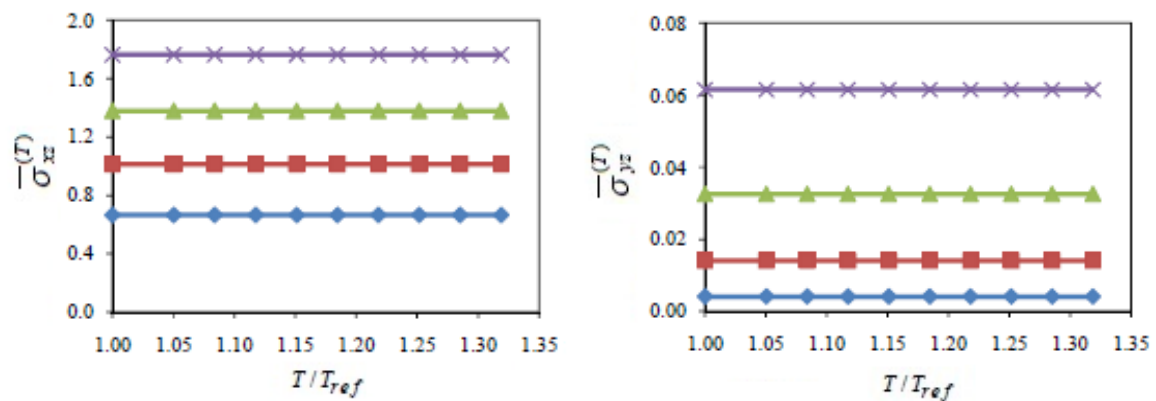
Interlaminar shear stresses,  $\bar{\sigma}_{xz}^{(T)}$  and  $\bar{\sigma}_{yz}^{(T)}$  and the in-plane shear stress,  $\bar{\sigma}_{xy}^{(T)}$  due to mechanical loading under the influence of thermal environment are examined. The results are presented as normalized quantities such that

$$(\bar{\sigma}_{xz}^{(T)}, \bar{\sigma}_{yz}^{(T)}, \bar{\sigma}_{xy}^{(T)}) = (\sigma_{xz}^{(T)}, \sigma_{yz}^{(T)}, \sigma_{xy}^{(T)}) / (T_{ref} \alpha_o E_o) \tag{4}$$

The variations in the normalized maximum interlaminar shear stresses,  $\bar{\sigma}_{xz}^{(T)}$  and  $\bar{\sigma}_{yz}^{(T)}$  for

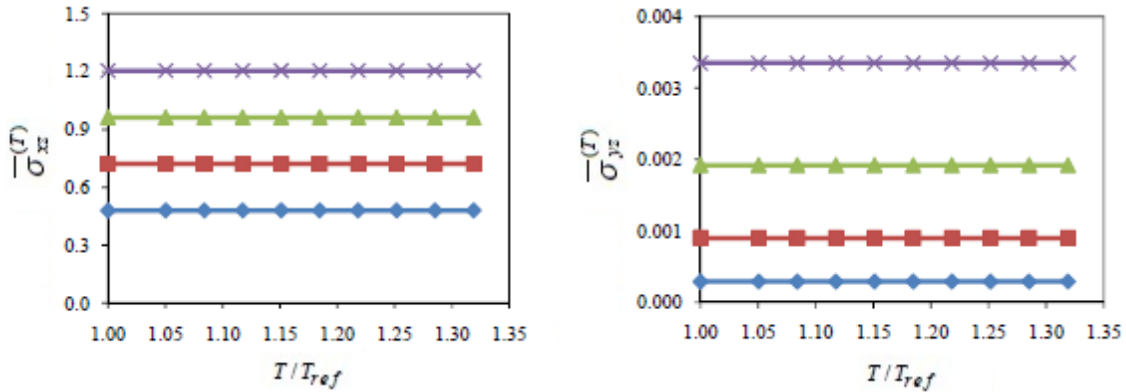


(a) Clamped-clamped boundary conditions



(b) Clamped-hinged boundary conditions

Fig. 4 Variation of normalised maximum interlaminar shear stresses (ILSS) along  $xz$  ( $\bar{\sigma}_{xz}^{(T)}$ ) and  $yz$  ( $\bar{\sigma}_{yz}^{(T)}$ ) planes of symmetric laminated composite beam with  $[0/90]_{4S}$  ply orientation under (a) clamped-clamped; (b) clamped-hinged; and (c) hinged-hinged boundary conditions



(c) Hinged-hinged boundary conditions

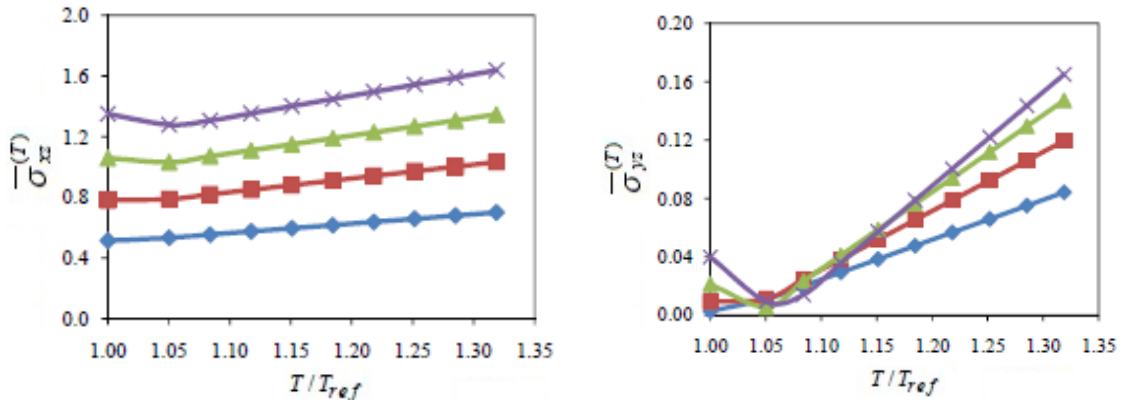
◆ L/H=20    ■ L/H=30    ▲ L/H=40    ✕ L/H=50

Fig. 4 Continued

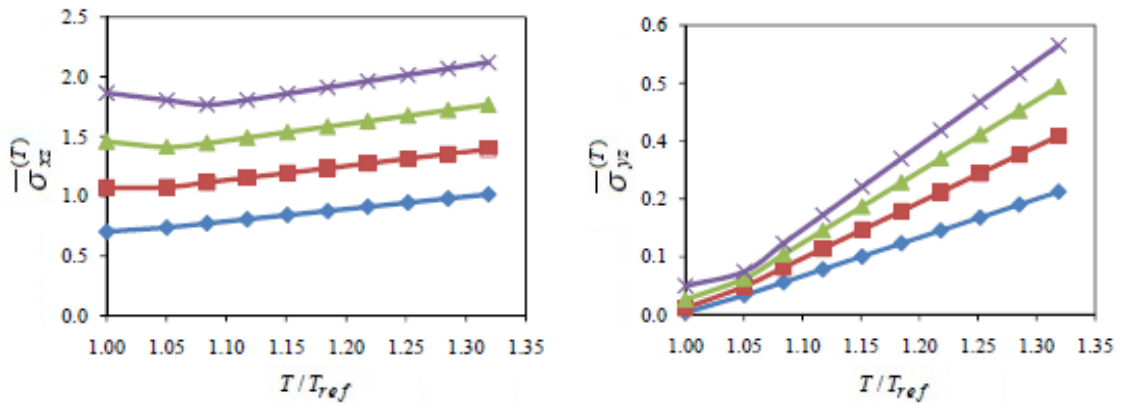
various ratios of length to thickness of composite laminated beam of stacking sequences  $[0/90]_{4S}$ , with application of mechanical loading 'p' under the influence of thermal environment are presented in Fig. 4. The results show that the variation in interlaminar stress is insignificant along both in  $xz$  and  $yz$  plane with increase in thermal environment in symmetric laminates. This may be due to the fact that the deformations above and below the mid plane of the symmetric and unidirectional laminated composite beams are balanced. It can also be seen that the interlaminar stresses along both  $xz$  and  $yz$  planes increase with increase in  $L/H$  ratio irrespective of end conditions and temperature distribution. This is obviously true as the bending moment increases with increase in length of the beam which yields increase in bending stresses. Furthermore, it is observed that the magnitude of the interlaminar stresses along  $xz$  plane is much higher than those along  $yz$  plane.

Figs. 5 and 6 present the variations in the normalised maximum interlaminar shear stresses,  $\bar{\sigma}_{xz}^{(T)}$  and  $\bar{\sigma}_{yz}^{(T)}$  for various ratios of length to thickness of composite laminated asymmetric and anti-symmetric beams of stacking sequences  $[0/90]_8$  and  $[0/(\pm 45)_7/0]$ , respectively, with application of mechanical loading of 1000 N/mm along  $y$  direction and the influence of thermal environment. It can be seen that the interlaminar stresses along  $xz$  and  $yz$  planes increase with increase in environmental temperature in asymmetric cross-ply laminated beam and anti-symmetric laminated beam irrespective of the end conditions. It can also be seen that as observed in symmetric laminates, the interlaminar stresses along both  $xz$  and  $yz$  planes increase with increase in  $L/H$  ratio irrespective of end conditions and temperature distribution. Furthermore, it is observed that the magnitude of the interlaminar stresses along  $xz$  plane is much higher than those along  $yz$  plane. It is also interesting to note that the interlaminar stresses along both  $xz$  plane and  $yz$  plane initially decrease marginally and then increase with increase in environmental temperature under clamped-clamped and clamped-hinged boundary conditions. This initial decrease in interlaminar shear stresses is steeper with higher  $L/H$  ratios. However this trend is not observed under hinged-hinged boundary conditions.

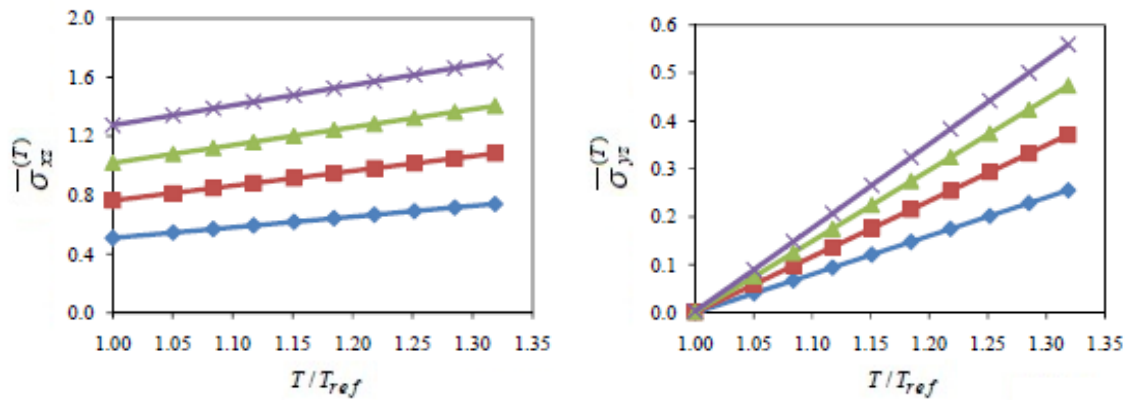
The variations in the normalised maximum in-plane shear stress,  $\bar{\sigma}_{xy}^{(T)}$  for various ratios of



(a) Clamped-clamped boundary conditions



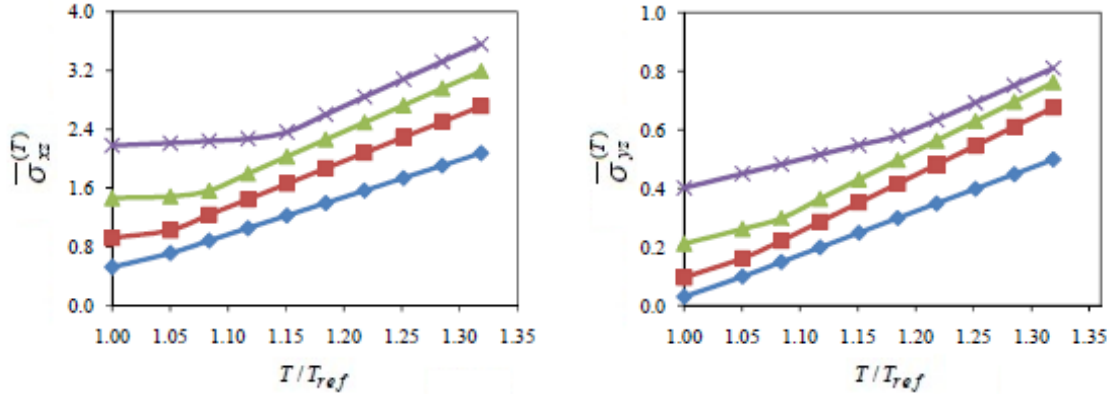
(b) Clamped-hinged boundary conditions



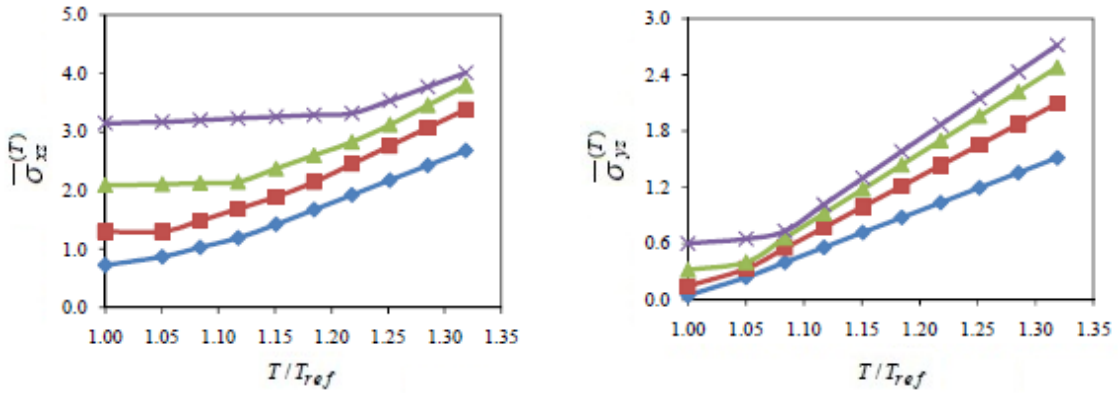
(c) Hinged-hinged boundary conditions

◆ L/H=20    ■ L/H=30    ▲ L/H=40    ✕ L/H=50

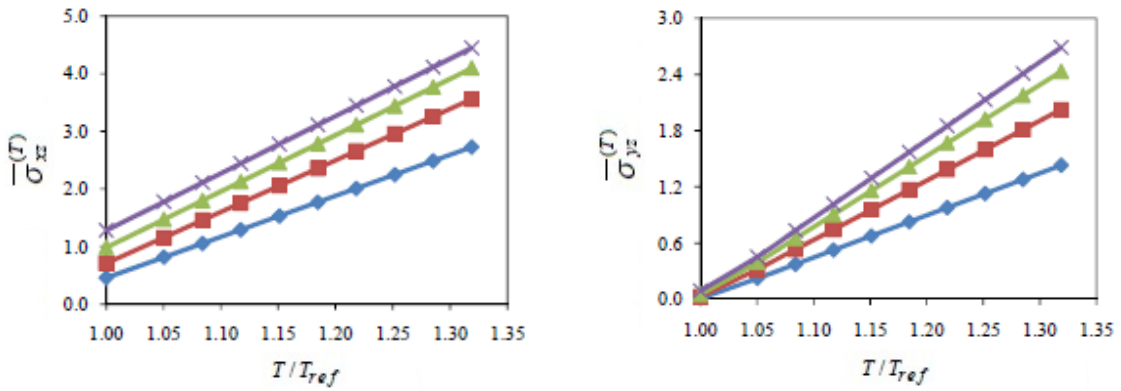
Fig. 5 Variation of normalised maximum interlaminar shear stresses (ILSS) along  $xz$  ( $\bar{\sigma}_{xz}^{(T)}$ ) and  $yz$  ( $\bar{\sigma}_{yz}^{(T)}$ ) planes of asymmetric laminated composite beam with  $[0/90]_8$  ply orientation under: (a) clamped-clamped; (b) clamped-hinged; and (c) hinged-hinged boundary conditions



(a) Clamped-clamped boundary conditions



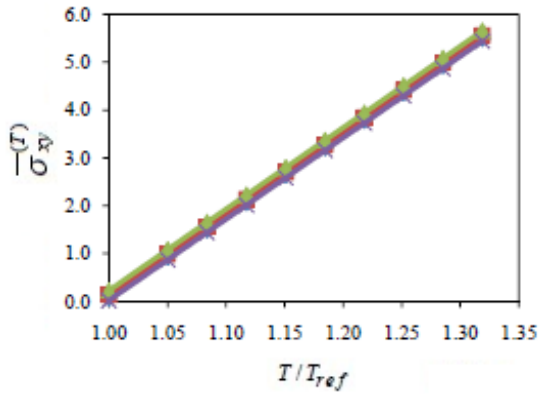
(b) Clamped-hinged boundary conditions



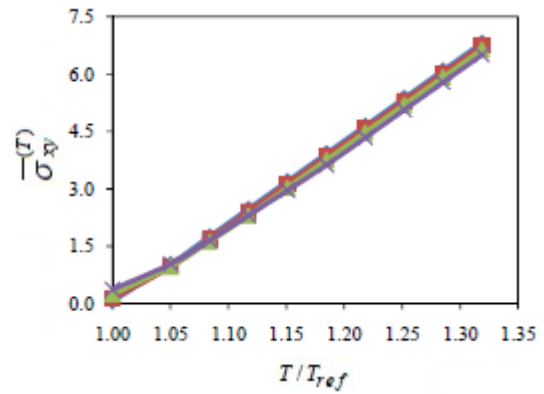
(c) Hinged-hinged boundary conditions

◆ L/H=20    ■ L/H=30    ▲ L/H=40    ✕ L/H=50

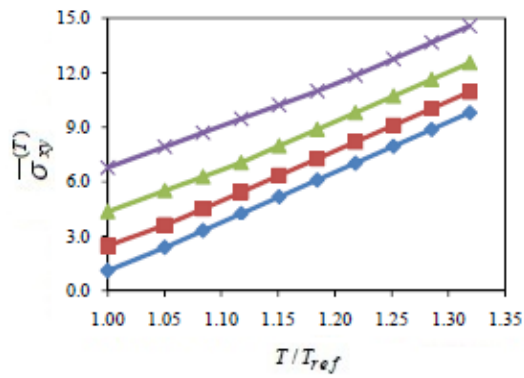
Fig. 6 Variation of normalised maximum interlaminar shear stresses (ILSS) along  $xz$  ( $\bar{\sigma}_{xz}^{(T)}$ ) and  $yz$  ( $\bar{\sigma}_{yz}^{(T)}$ ) planes of anti-symmetric laminated composite beam with  $[0/(\pm 45)_7/0]$  ply orientation under: (a) clamped-clamped; (b) clamped-hinged; and (c) hinged-hinged boundary conditions



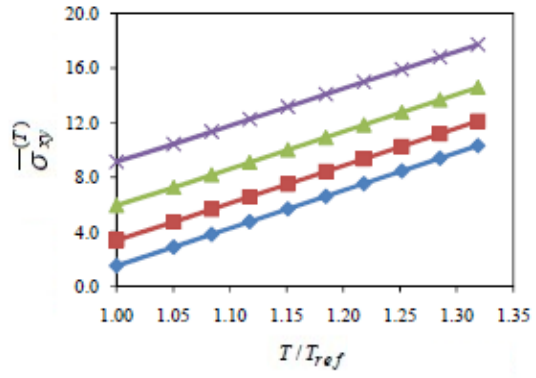
(a) Beam of  $[0/90]_{4S}$  ply orientation under clamped-hinged boundary condition



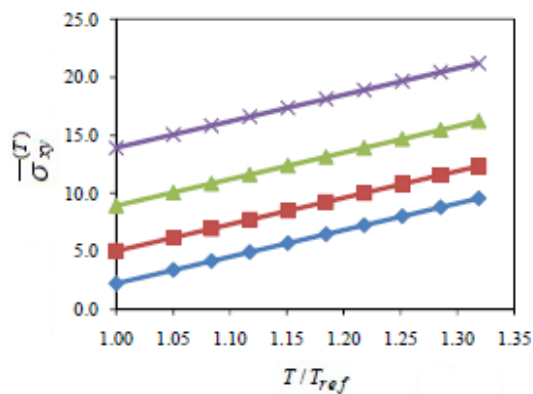
(b) Beam of  $[0/90]_8$  ply orientation under clamped-hinged boundary condition



(c) Beam of  $[0/(\pm 45)_7/0]$  ply orientation under clamped-clamped boundary condition



(d) Beam of  $[0/(\pm 45)_7/0]$  ply orientation under clamped-hinged boundary condition



(e) Beam of  $[0/(\pm 45)_7/0]$  ply orientation under hinged-hinged boundary condition

◆  $L/H=20$     ■  $L/H=30$     ▲  $L/H=40$     ✕  $L/H=50$

Fig. 7 Variation of normalised maximum in-plane shear stress ( $\bar{\sigma}_{xy}^{(T)}$ ) along  $xy$  plane of laminated composite beam with various ply orientation under the influence of thermal environment

length to thickness of the beam of stacking sequences  $[0/90]_{4S}$ ,  $[0/90]_8$ , and  $[0/(\pm 45)_7/0]$  due to identical mechanical loading ‘ $p$ ’, under the influence of thermal environment are analyzed and presented in Fig. 7.

The normalized maximum interlaminar shear stresses,  $\bar{\sigma}_{xz}^{(T)}$  and  $\bar{\sigma}_{yz}^{(T)}$  and the in-plane shear stress,  $\bar{\sigma}_{xy}^{(T)}$  for various ratios of length to thickness of the unidirectional composite laminated beam of stacking sequences  $[0]_{16}$ ,  $[45]_{16}$  and  $[90]_{16}$  due to identical mechanical loading ‘ $p$ ’ under the influence of thermal environment are further investigated and presented in Tables 3-6 for various  $L/H$  ratios. The results show that the variation in normalised interlaminar shear stresses,  $\bar{\sigma}_{xz}^{(T)}$  and  $\bar{\sigma}_{yz}^{(T)}$  are insignificant as in symmetric cross-ply laminated composite beam of stacking sequence  $[0/90]_{4S}$ . However this insignificant variation in interlaminar stresses is coupled with substantial variation in in-plane stresses at elevated thermal environment.

It can also be observed that in symmetric laminated beam  $[0/90]_{4S}$ , and unidirectional laminated beams  $[0]_{16}$ ,  $[45]_{16}$  and  $[90]_{16}$ , interlaminar stresses along both  $xz$  plane and  $yz$  plane are higher under clamped-hinged boundary conditions compared to that under clamped-clamped and hinged-hinged boundary conditions irrespective of  $L/H$  ratios. This is evident from Fig. 4 and Tables 3-6.

Another interesting pattern observed in anti-symmetric composite laminated beam  $[0/(\pm 45)_7/0]$ , shown in Fig. 6, is that the rate of change of interlaminar stresses along both  $xz$  plane and  $yz$  plane is comparatively lesser for initial increase in environmental temperature than for higher

Table 3 Comparison of results of symmetric composite laminated beams of stacking sequences  $[0]_{16}$ ,  $[45]_{16}$  and  $[90]_{16}$  for  $L/H = 20$  under the influence of thermal environment

Ply →	[0] <sub>16</sub>			[45] <sub>16</sub>			[90] <sub>16</sub>		
B.C.*	$\bar{\sigma}_{xy}^{(T)}$	$\bar{\sigma}_{yz}^{(T)}$	$\bar{\sigma}_{xz}^{(T)}$	$\bar{\sigma}_{xy}^{(T)}$	$\bar{\sigma}_{yz}^{(T)}$	$\bar{\sigma}_{xz}^{(T)}$	$\bar{\sigma}_{xy}^{(T)}$	$\bar{\sigma}_{yz}^{(T)}$	$\bar{\sigma}_{xz}^{(T)}$
$T/T_{ref} = 1.0$									
CC	0.1008	0.0070	0.5209	0.1493	0.3725	0.3725	0.1008	0.5209	0.0070
CH	0.1485	0.0102	0.7139	0.2240	0.5140	0.5140	0.1485	0.7139	0.0102
HH	0.0041	0.0009	0.5062	0.0026	0.3577	0.3577	0.0041	0.5062	0.0009
$T/T_{ref} = 1.1$									
CC	13.7022	0.0070	0.5209	0.4924	0.3725	0.3725	13.7022	0.5209	0.0070
CH	13.7499	0.0102	0.7139	0.5671	0.5140	0.5140	13.7499	0.7139	0.0102
HH	13.6023	0.0009	0.5062	0.3436	0.3577	0.3577	13.6023	0.5062	0.0009
$T/T_{ref} = 1.2$									
CC	27.3036	0.0070	0.5209	0.8354	0.3725	0.3725	27.3036	0.5209	0.0070
CH	27.3513	0.0102	0.7139	0.9102	0.5140	0.5140	27.3513	0.7139	0.0102
HH	27.2040	0.0009	0.5062	0.6867	0.3577	0.3577	27.2040	0.5062	0.0009
$T/T_{ref} = 1.3$									
CC	40.9049	0.0070	0.5209	1.1785	0.3725	0.3725	40.9049	0.5209	0.0070
CH	40.9526	0.0102	0.7139	1.2533	0.5140	0.5140	40.9526	0.7139	0.0102
HH	40.8056	0.0009	0.5062	1.0298	0.3577	0.3577	40.8056	0.5062	0.0009

\* CC - Clamped-Clamped, CH - Clamped-Hinged and HH - Hinged-Hinged boundary conditions

Table 4 Comparison of results of symmetric composite laminated beams of stacking sequences  $[0]_{16}$ ,  $[45]_{16}$  and  $[90]_{16}$  for  $L/H=30$  under the influence of thermal environment

Ply →	$[0]_{16}$			$[45]_{16}$			$[90]_{16}$		
B.C.*	$\bar{\sigma}_{xy}^{(T)}$	$\bar{\sigma}_{yz}^{(T)}$	$\bar{\sigma}_{xz}^{(T)}$	$\bar{\sigma}_{xy}^{(T)}$	$\bar{\sigma}_{yz}^{(T)}$	$\bar{\sigma}_{xz}^{(T)}$	$\bar{\sigma}_{xy}^{(T)}$	$\bar{\sigma}_{yz}^{(T)}$	$\bar{\sigma}_{xz}^{(T)}$
$T/T_{ref} = 1.0$									
CC	0.2208	0.0222	0.8115	0.3411	0.6050	0.6050	0.2208	0.8115	0.0222
CH	0.3296	0.0330	1.1200	0.5128	0.8410	0.8410	0.3296	1.1200	0.0330
HH	0.0105	0.0028	0.7630	0.0090	0.5393	0.5393	0.0105	0.7630	0.0028
$T/T_{ref} = 1.1$									
CC	13.8221	0.0222	0.8115	0.6842	0.6050	0.6050	13.8221	0.8115	0.0222
CH	13.9309	0.0330	1.1200	0.8559	0.8410	0.8410	13.9309	1.1200	0.0330
HH	13.6058	0.0028	0.7630	0.3472	0.5393	0.5393	13.6058	0.7630	0.0028
$T/T_{ref} = 1.2$									
CC	27.4235	0.0222	0.8115	1.0273	0.6050	0.6050	27.4235	0.8115	0.0222
CH	27.5323	0.0330	1.1200	1.1990	0.8410	0.8410	27.5323	1.1200	0.0330
HH	27.2075	0.0028	0.7630	0.6903	0.5393	0.5393	27.2075	0.7630	0.0028
$T/T_{ref} = 1.3$									
CC	41.0248	0.0222	0.8115	1.3704	0.6050	0.6050	41.0248	0.8115	0.0222
CH	41.1336	0.0330	1.1200	1.5420	0.8410	0.8410	41.1336	1.1200	0.0330
HH	40.8091	0.0028	0.7630	1.0334	0.5393	0.5393	40.8091	0.7630	0.0028

Table 5 Comparison of results of symmetric composite laminated beams of stacking sequences  $[0]_{16}$ ,  $[45]_{16}$  and  $[90]_{16}$  for  $L/H=40$  under the influence of thermal environment

Ply →	$[0]_{16}$			$[45]_{16}$			$[90]_{16}$		
B. C.*	$\bar{\sigma}_{xy}^{(T)}$	$\bar{\sigma}_{yz}^{(T)}$	$\bar{\sigma}_{xz}^{(T)}$	$\bar{\sigma}_{xy}^{(T)}$	$\bar{\sigma}_{yz}^{(T)}$	$\bar{\sigma}_{xz}^{(T)}$	$\bar{\sigma}_{xy}^{(T)}$	$\bar{\sigma}_{yz}^{(T)}$	$\bar{\sigma}_{xz}^{(T)}$
$T/T_{ref} = 1.0$									
CC	0.3792	0.0490	1.1324	0.6175	0.8709	0.8709	0.3792	1.1324	0.0490
CH	0.5690	0.0731	1.5714	0.9288	1.2181	1.2181	0.5690	1.5714	0.0731
HH	0.0232	0.0071	1.0219	0.0218	0.7229	0.7229	0.0232	1.0219	0.0071
$T/T_{ref} = 1.1$									
CC	13.9806	0.0490	1.1324	0.9606	0.8709	0.8709	13.9806	1.1324	0.0490
CH	14.1704	0.0731	1.5714	1.2719	1.2181	1.2181	14.1704	1.5714	0.0731
HH	13.6142	0.0071	1.0219	0.3557	0.7229	0.7229	13.6142	1.0219	0.0071
$T/T_{ref} = 1.2$									
CC	27.5819	0.0490	1.1324	1.3037	0.8709	0.8709	27.5819	1.1324	0.0490
CH	27.7717	0.0731	1.5714	1.6150	1.2181	1.2181	27.7717	1.5714	0.0731
HH	27.2159	0.0071	1.0219	0.6988	0.7229	0.7229	27.2159	1.0219	0.0071

Table 5 Continued

Ply →	[0] <sub>16</sub>			[45] <sub>16</sub>			[90] <sub>16</sub>		
B. C.*	$\bar{\sigma}_{xy}^{(T)}$	$\bar{\sigma}_{yz}^{(T)}$	$\bar{\sigma}_{xz}^{(T)}$	$\bar{\sigma}_{xy}^{(T)}$	$\bar{\sigma}_{yz}^{(T)}$	$\bar{\sigma}_{xz}^{(T)}$	$\bar{\sigma}_{xy}^{(T)}$	$\bar{\sigma}_{yz}^{(T)}$	$\bar{\sigma}_{xz}^{(T)}$
$T/T_{ref} = 1.3$									
CC	41.1833	0.0490	1.1324	1.6467	0.8709	0.8709	41.1833	1.1324	0.0490
CH	41.3731	0.0731	1.5714	1.9580	1.2181	1.2181	41.3731	1.5714	0.0731
HH	40.8176	0.0071	1.0219	1.0419	0.7229	0.7229	40.8176	1.0219	0.0071

Table 6 Comparison of results of symmetric composite laminated beams of stacking sequences [0]<sub>16</sub>, [45]<sub>16</sub> and [90]<sub>16</sub> for  $L/H=50$  under the influence of thermal environment

Ply →	[0] <sub>16</sub>			[45] <sub>16</sub>			[90] <sub>16</sub>		
B. C.*	$\bar{\sigma}_{xy}^{(T)}$	$\bar{\sigma}_{yz}^{(T)}$	$\bar{\sigma}_{xz}^{(T)}$	$\bar{\sigma}_{xy}^{(T)}$	$\bar{\sigma}_{yz}^{(T)}$	$\bar{\sigma}_{xz}^{(T)}$	$\bar{\sigma}_{xy}^{(T)}$	$\bar{\sigma}_{yz}^{(T)}$	$\bar{\sigma}_{xz}^{(T)}$
$T/T_{ref} = 1.0$									
CC	0.5700	0.0880	1.4862	0.9825	1.1796	1.1796	0.5700	1.4862	0.0880
CH	0.8576	0.1316	2.0723	1.4786	1.6595	1.6595	0.8576	2.0723	0.1316
HH	0.0457	0.0136	1.2821	0.0423	0.9085	0.9085	0.0457	1.2821	0.0136
$T/T_{ref} = 1.1$									
CC	14.1713	0.0880	1.4862	1.3256	1.1796	1.1796	14.1713	1.4862	0.0880
CH	14.4589	0.1316	2.0723	1.8217	1.6595	1.6595	14.4589	2.0723	0.1316
HH	13.6294	0.0136	1.2821	0.3704	0.9085	0.9085	13.6294	1.2821	0.0136
$T/T_{ref} = 1.2$									
CC	27.7727	0.0880	1.4862	1.6687	1.1796	1.1796	27.7727	1.4862	0.0880
CH	28.0603	0.1316	2.0723	2.1648	1.6595	1.6595	28.0603	2.0723	0.1316
HH	27.2310	0.0136	1.2821	0.7135	0.9085	0.9085	27.2310	1.2821	0.0136
$T/T_{ref} = 1.3$									
CC	41.3740	0.0880	1.4862	2.0118	1.1796	1.1796	41.3740	1.4862	0.0880
CH	41.6616	0.1316	2.0723	2.5079	1.6595	1.6595	41.6616	2.0723	0.1316
HH	40.8327	0.0136	1.2821	1.0566	0.9085	0.9085	40.8327	1.2821	0.0136

environmental temperatures under clamped-clamped and clamped-hinged boundary conditions.

However, the rate of change of interlaminar stresses along both  $xz$  plane and  $yz$  plane with increase in environmental temperature are higher under hinged-hinged boundary conditions for same  $L/H$  ratios in asymmetric and anti-symmetric cross-ply laminated composite beams.

It is interesting to note that the interlaminar stresses along  $xz$  plane and  $yz$  planes are complementary such that the interlaminar stresses along  $xz$  plane is higher than that along  $yz$  planes for laminated beams with predominantly more  $0^\circ$  plies and the inverse for laminated beams with more  $90^\circ$  plies irrespective of  $L/H$  ratios and boundary conditions. Following the similar

pattern, the interlaminar stresses along both  $xz$  plane and  $yz$  planes are equal in laminated beam with the stacking sequence of  $[45]_{16}$  under identical mechanical loading and environmental temperature with identical boundary conditions.

It is inferred that the effect of thermal environment on the interlaminar shear stresses in carbon-epoxy fiber reinforced composite laminated beams is increasing in the order of symmetric cross-ply laminate, unidirectional laminate, asymmetric cross-ply laminate and anti-symmetric laminate depending upon the boundary conditions. However the inplane stresses are the lowest in symmetric cross-ply laminated composite beam and highest in unidirectional laminated composite beam.

## **6. Conclusions**

In the present study the combined effect of thermal environment and mechanical loadings on the interlaminar shear stresses of both thin and moderately thick composite laminated beams are numerically analyzed. The validity of the finite element analysis is demonstrated by comparing the results in terms of interlaminar shear stress identified from experimental test results. Various parametric studies are also performed to investigate the effect of thermal environment on interlaminar stresses generated in symmetric, anti-symmetric, asymmetric, cross-ply, unidirectional and balanced composite laminated beams of different stacking sequences with identical mechanical loadings under different boundary conditions. It is observed that the elevated thermal environment leads to higher interlaminar shear stresses varying with the stacking sequence, length to thickness ratio, ply orientations and boundary conditions of the composite laminated beams. It is also shown that the interlaminar stresses along  $xz$  and  $yz$  planes increase with increase in environmental temperature in anti-symmetric and asymmetric laminated beams, under various boundary conditions. However, similar trends could not be observed in symmetric and unidirectional laminated beams. The results also show that the variation in interlaminar stress is almost negligible along both in  $xz$  and  $yz$  plane with increase in thermal environment in symmetric and unidirectional laminates irrespective of length to thickness ratios under different boundary conditions.

It is also observed that the interlaminar stresses along  $xz$  plane and  $yz$  planes are complementary irrespective of ply orientations,  $L/H$  ratios and boundary conditions. On similar pattern, for the laminated beam with the stacking sequence of  $[45]_{16}$ , the interlaminar stresses along both  $xz$  plane and  $yz$  planes are equal.

It is also observed that the effect of thermal environment on the interlaminar shear stresses in carbon-epoxy fiber reinforced composite laminated beams are increasing in the order of symmetric cross-ply laminate, unidirectional laminate, asymmetric cross-ply laminate and anti-symmetric laminate. The interlaminar shear stresses are higher in thinner composite laminated beams compared to those obtained in thicker composite laminated beams irrespective of environmental temperatures and the laminate stacking sequence, ply-orientation and boundary conditions.

It was also shown that the interlaminar shear stresses are significantly influenced by the combined effect of elevated thermal environment and mechanical loadings in addition to the boundary conditions. It was also observed that the interlaminar stresses are higher under clamped-hinged and hinged-hinged boundary conditions compared to those of under clamped-clamped boundary conditions. However, the interlaminar stresses are higher under clamped-hinged boundary conditions compared to clamped-clamped and hinged-hinged boundary conditions for

unidirectional laminates with fiber orientation of  $0^\circ$ ,  $45^\circ$  and  $90^\circ$ .

It can be concluded that significant variation in interlaminar shear stresses and in-plane stresses could be observed under elevated environmental temperatures in addition to the mechanical loadings.

## References

- Aydogdu, M. (2007), "Thermal buckling analysis of cross-ply laminated composite beams with general boundary conditions", *Compos. Sci. Technol.*, **67**(6), 1096-1104.
- Becker, W., Jin, P.P. and Lindemann, J. (2001), "The free-corner effect in thermally loaded laminates", *Compos. Struct.*, **52**(1), 97-102.
- Bhaskar, K. and Kaushik, B. (2004), "Simple and exact series solutions for flexure of orthotropic rectangular plates with any combination of clamped and simply supported edges", *Compos. Struct.*, **63**(1), 63-68.
- Cho, M. and Kim, H.S. (2000), "Iterative free-edge stress analysis of composite laminates under extension, bending, twisting and thermal loadings", *Int. J. Solid. Struct.*, **37**(3), 435-459.
- Cho, M. and Oh, J. (2003), "Higher order zig-zag plate theory under thermo-electric-mechanical loads combined", *Compos.: Part B*, **34**(1), 67-82.
- Cho, M. and Oh, J. (2004), "Higher order zig-zag theory for fully coupled thermo-electric-mechanical smart composite plates", *Int. J. Solid. Struct.*, **41**(5-6), 1331-1356.
- Gatto, A., Mattioni, F. and Friswell, M.I. (2009), "Experimental investigation of bistable winglets to enhance wing lift takeoff capability", *J. Aircraft*, **46**(2), 647-655.
- Gayen, D. and Roy, T. (2013), "Hygro-Thermal Effects on Stress Analysis of Tapered Laminated Composite Beam", *Int. J. Compos. Mater.*, **3**(3), 46-55.
- Hu, E.Z., Soutis, C. and Edge, E.C. (1997), "Interlaminar stresses in composite laminates with Interlaminar stresses in composite a circular hole," *Compos. Struct.*, **37**(2), 223-232.
- Kassapoglou, C. (1990), "Determination of Interlaminar Stresses in Composite Laminates under Combined Loads", *J. Reinf. Plast. Compos.*, **9**(1), 33-58.
- Kress, G., Roos, R., Barbezat, M., Dransfeld, C. and Ermann, P. (2005), "Model for interlaminar normal stress in singly curved laminates", *Compos. Struct.*, **69**(4), 458-469.
- Lee, Y.W. (1994), "Interlaminar stress analysis of composite laminates using a sublaminar/layer model" *Int. J. Solid. Struct.*, **31**(11), 1549-1564.
- Lee, C.Y. and Liu, D. (1992), "An interlaminar stress continuity theory for laminated composite analysis", *Comput. Struct.*, **42**(1), 69-78.
- Matsunaga, H. (2002), "Interlaminar stress analysis of laminated composite beams according to global higher-order deformation theories", *Compos. Struct.*, **55**(1), 105-114.
- Matsunaga, H. (2003), "Interlaminar stress analysis of laminated composite and sandwich circular arches subjected to thermal/mechanical loading", *Compos. Struct.*, **60**(3), 345-358.
- Matsunaga, H. (2004), "A comparison between 2-D single-layer and 3-D layerwise theories for computing interlaminar stresses of laminated composite and sandwich plates subjected to thermal loadings", *Compos. Struct.*, **64**(2), 161-177.
- Murthy, M.V.V.S., Mahapatra, D.R., Badarinarayana, K. and Gopalakrishnan, S. (2005), "A refined higher order finite element for asymmetric composite beams", *Compos. Struct.*, **67**(1), 27-35.
- Oh, J. and Cho, M. (2004), "A finite element based on cubic zig-zag plate theory for the prediction of thermo-electric-mechanical behaviours", *Int. J. Solid. Struct.*, **41**(5-6), 1357-1375.
- Pagano, N.J. (1969), "Exact solutions for composite laminates in cylindrical bending", *J. Compos. Mater.*, **3**(3), 398-411.
- Plagianakos, T.S. and Saravanos, D.A. (2009), "Higher-order layerwise laminate theory for the prediction of interlaminar shear stresses in thick composite and sandwich composite plates", *Compos. Struct.*, **87**(1), 23-35.

- Rand, O. (1998), "Interlaminar shear stresses in solid composite beams using a complete out-of-plane shear deformation model", *Compos. Struct.*, **66**(6), 713-723.
- Rolfes, R. and Rohwer, K. (2000), "Integrated thermal and mechanical analysis of composite plates and shells", *Compos. Sci. Technol.*, **60**(11), 2097-2106.
- Salamon, N.J. (1978), "Interlaminar stresses in a layered composite Laminate in bending", *Fibre Sci. Technol.*, **11**(4), 305-317.
- Shariyat, M. (2010), "A generalized high-order global-local plate theory for nonlinear bending and buckling analyses of imperfect sandwich plates subjected to thermo-mechanical loads", *Compos. Struct.*, **92**(1), 130-143.
- Tahani, M. (2007), "Analysis of laminated composite beams using layerwise displacement theories", *Compos. Struct.*, **79**(4), 535-547.
- Tong, J.W., Xie, M.Y. and Shen, M. (2004), "The interlaminar stresses of symmetric composite laminates", *J. Reinf. Plast. Compos.*, **23**(10), 1023-1029.
- Vidal, P. and Polit, O. (2008), "A family of sinus finite elements for the analysis of rectangular laminated beams", *Compos. Struct.*, **84**(1), 56-72.
- Vidal, P. and Polit, O. (2009), "A refined sine-based finite element with transverse normal deformation for the analysis of laminated beams under thermo mechanical loads", *J. Mech. Mater. Struct.*, **4**(6), 1127-1155.
- Wu, C.P. and Kuo, H.C. (1993), "An interlaminar stress mixed finite element method for the analysis of thick laminated composite plates", *Compos. Struct.*, **24**(1), 29-42.
- Wu, H. and Yan, X. (2005), "Interlaminar stress modeling of composite laminates with finite element method", *J. Reinf. Plast. Compos.*, **24**(3), 130-143.